Electronic Supplementary Material (ESI) for CrystEngComm

Controlled synthesis of $Mn_xFe_{1-x}O$ concave nanocubes and highly branched cubic mesocrystals

Zhenhu Li, Yurong Ma* and Limin Qi*

Supporting Information

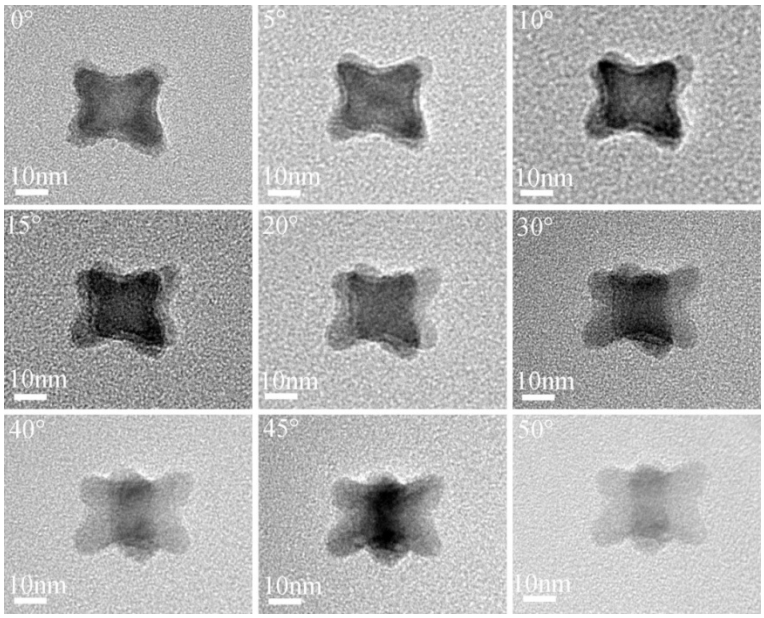

Fig. S1. TEM images of one of the $Mn_{0.15}Fe_{0.85}O$ concave nanocubes (Fig. 1) recorded after tilting the sample holder to different angles.

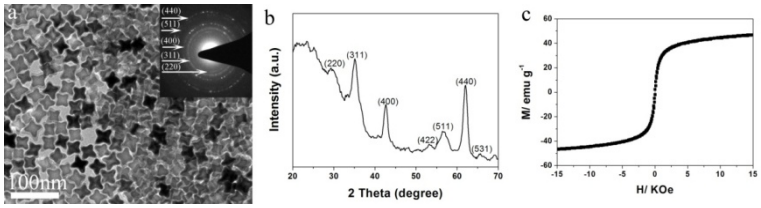

Fig. S2. Characterizations on the $Mn_xFe_{3-x}O_4$ concave nanocubes obtained while the $Mn_{0.15}Fe_{0.85}O$ concave nanocubes were exposed to air for 2 hours at 200 °C. (a) TEM image and corresponding SAED pattern, (b) XRD pattern, and (c) Magnetic hysteresis loops.

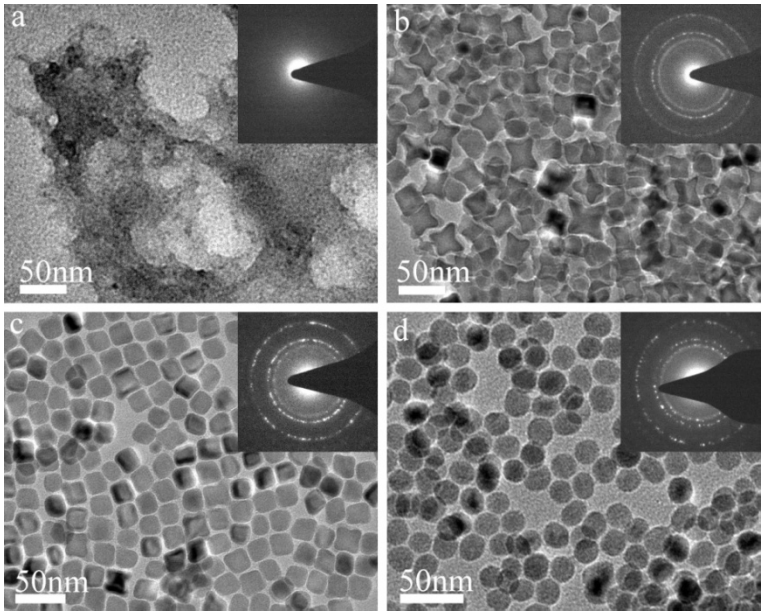

Fig. S3 TEM images of $Mn_{0.15}Fe_{0.85}O$ NPs obtained with different volume ratios of OA to OAm ($R_{OA/OAm}$) while remaining the total volume of OA and OAm as 10 mL. The insets show the corresponding SAED patterns. The $R_{OA/OAm}$ values are as follows: (a) 1.25, (b) 0.9, (c) 0.8, (d) 0.67.

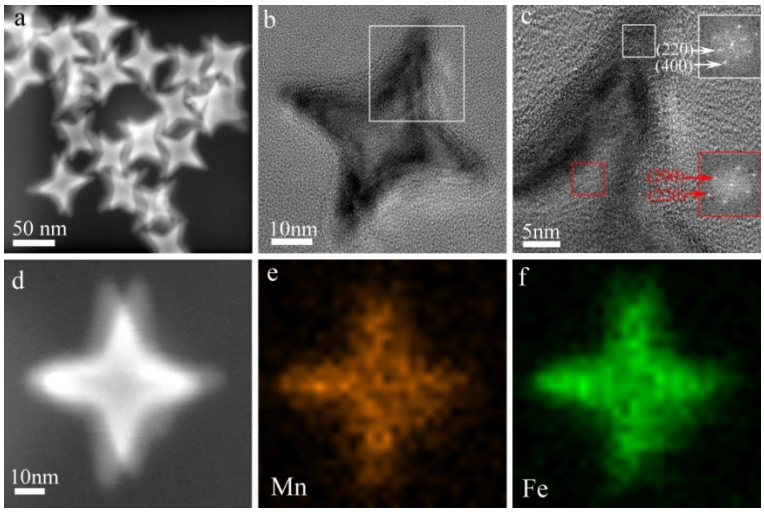

Fig. S4 Characterizations in details on $Mn_{0.15}Fe_{0.85}O$ concave nanocubes obtained with the concentration sum of metal precursors 0.18 mol/L and heating rate of 5 °C/min (Fig. 3c), (a) TEM, (b, c) high resolution TEM images, (Inset: FFTs of the marked areas corresponding to the red and white boxes, respectively) (d) a HAADF-STEM image, and (e, f) Mn and Fe mappings of a $Mn_{0.15}Fe_{0.85}O$ concave nanocubes.

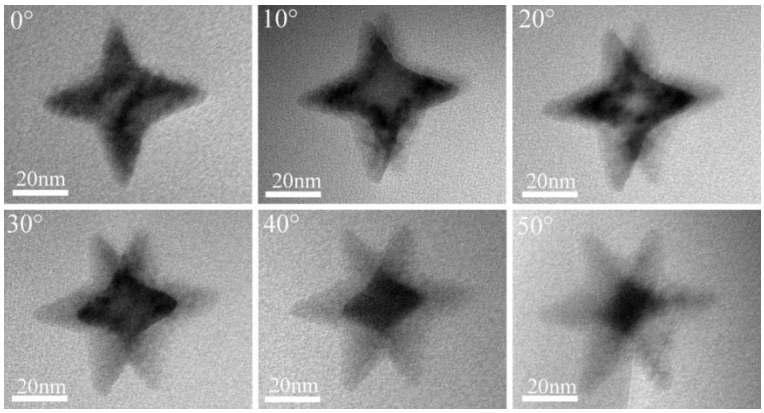

Fig. S5 TEM images of one of the $Mn_{0.15}Fe_{0.85}O$ concave nanocubes obtained with the concentration sum of metal precursors 0.18 mol/L and heating rate of 5 °C/min (Fig. 3c) recorded after tilting the sample holder in-situ to different angles.

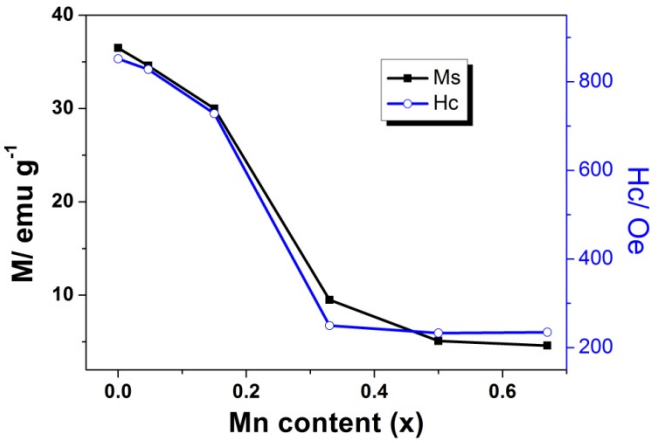

Fig. S6 The relation of the Mn contents (x) and the saturation magnetization (Ms) and coercive field values (Hc) of the obtained $Mn_xFe_{1-x}O$ nanoparticles characterized at 2 T and 5 K.

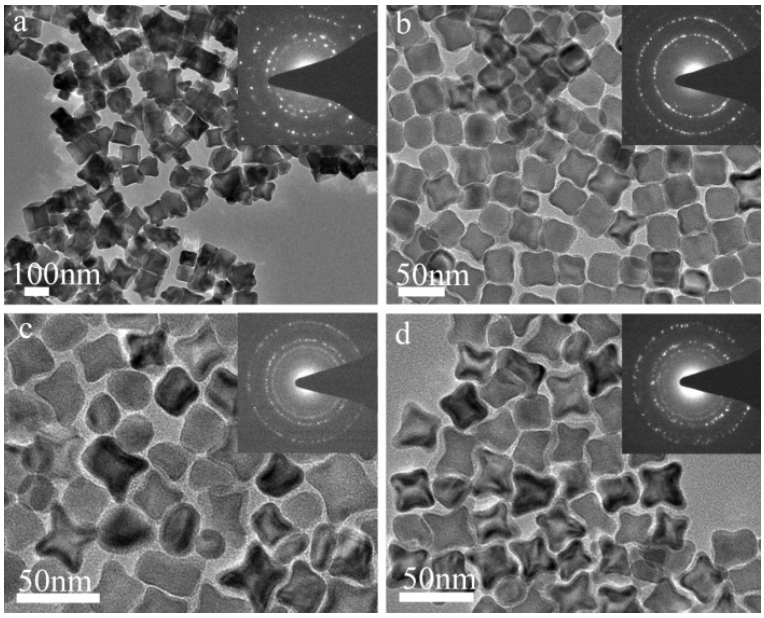

Fig. S7 TEM images of $Mn_{0.15}Fe_{0.85}O$ nanoparticles obtained when the heating time for the first step heating process at 200°C was varied from 0 to 60 min while keeping the second step heating time at 300 °C to be 60 min. The insets show the corresponding SAED patterns. (a) 0, (b)10 min, (c)30 min, (d) 40 min.

Scheme S1. Schematic illustration of the formation mechanism for the $Mn_xFe_{1-x}O$ concave nanocubes.

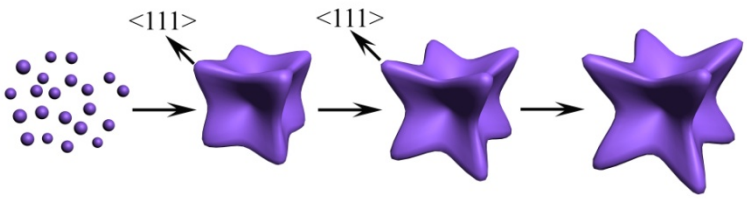

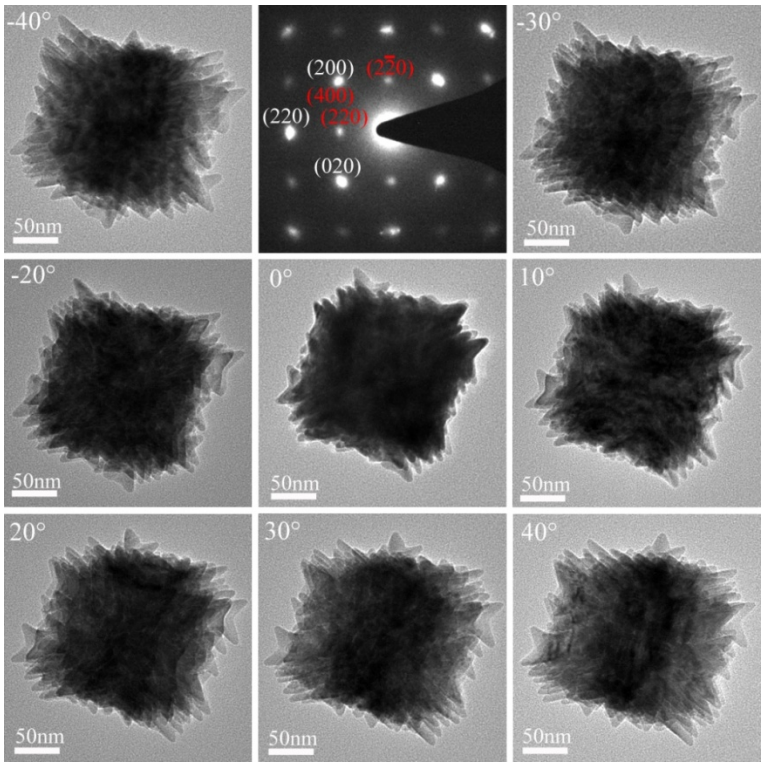

Fig. S8. TEM images of one of the highly branched cubic $Mn_{0.15}Fe_{0.85}O$ mesocrystals (Fig. 7) recorded after tilting the sample holder to different angles. The SAED pattern related to the image obtained at -40º shows crystal facets indexes in white and red corresponding to $Mn_xFe_{1-x}O$ rock salt phase and $Mn_xFe_{3-x}O_4$ spinel phases, respectively).

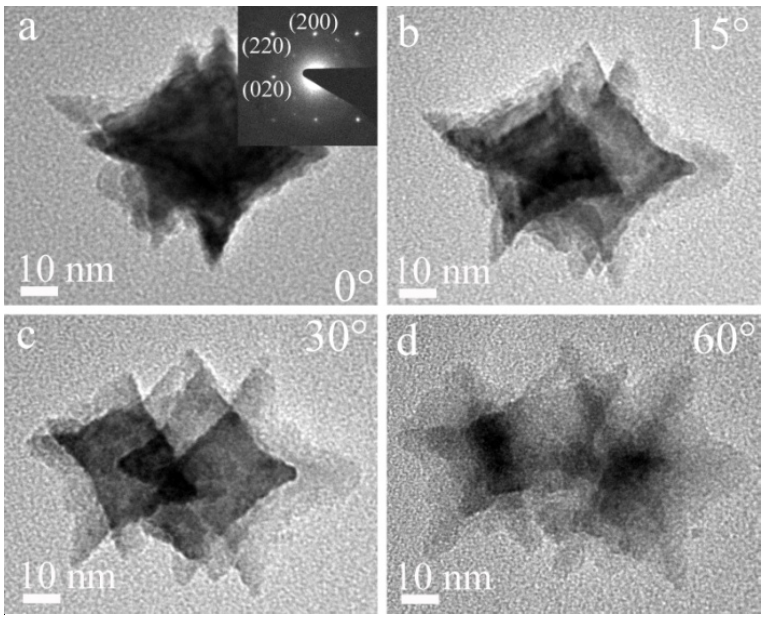

Fig. S9. TEM images of one of the highly branched cubic $Mn_{0.15}Fe_{0.85}O$ mesocrystals after aging at 300 °C for 30 min (Fig. 8c) recorded after tilting the sample holder to different angles. The inset in (a) shows the SAED pattern

corresponding to planes of $Mn_xFe_{1-x}O$ rock salt phase.

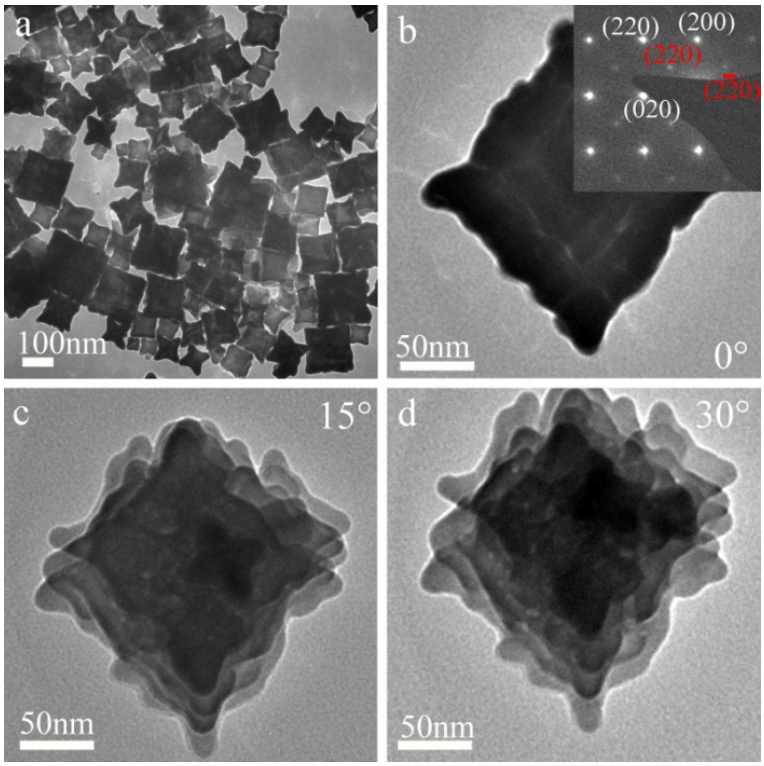

Fig. S10 TEM images of the highly branched cubic $Mn_{0.15}Fe_{0.85}O$ mesocrystals after aging at 300 °C for 120 min. (b-d) TEM of one $Mn_{0.15}Fe_{0.85}O$ mesocrystal recorded after tilting the sample holder to different angles. The inset in (b) shows the SAED pattern with crystal facets indexes in white and red corresponding to $Mn_xFe_{1-x}O$ rock salt phase and $Mn_xFe_{3-x}O_4$ spinel phases, respectively.

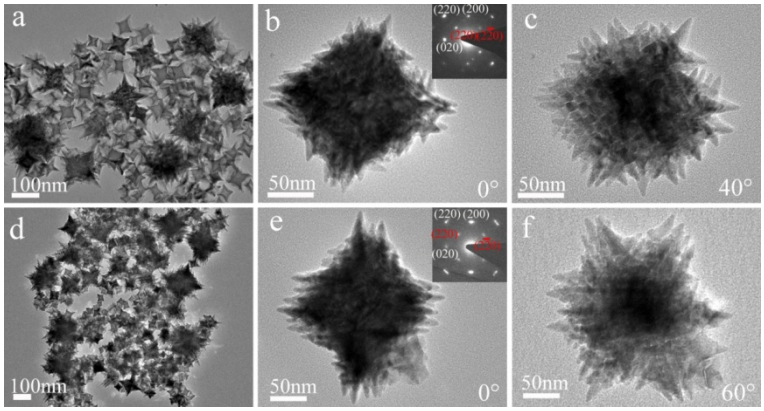

Fig. S11 TEM images of the highly branched cubic $Mn_{0.15}Fe_{0.85}O$ mesocrystals obtained in the presence of different amounts of 1-octadecene, (a-c) 2.5 ml, (d-f) 7.5 ml. The insets in (b) and (e) show the relative SAED patterns with crystal facets indexes in white and red corresponding to $Mn_xFe_{1-x}O$ rock salt phase and $Mn_xFe_{3-x}O_4$

spinel phases, respectively. The images in (c) and (f) were obtained after tilting the mesocrystals in (b) and (e) to different angles, respectively.